ISSN 1063-7729, Astronomy Reports, 2011, Vol. 55, No. 12, pp. 1086–1095. © Pleiades Publishing, Ltd., 2011.
Original Russian Text © I.D. Litovchenko, A.V. Alakoz, I.E. Val'tts, G.M. Larionov, 2011, published in Astronomicheskii Zhurnal, 2011, Vol. 88, No. 12, pp. 1177–1187.

Search for Class I Methanol Maser Emission in Various Types of Objects in the Interstellar Medium

I. D. Litovchenko*, A. V. Alakoz, I. E. Val'tts, and G. M. Larionov

Astro Space Center, Lebedev Physical Institute, Russian Academy of Sciences, Profsoyuznaya ul. 84/32, Moscow, 117997 Russia

Received March 18, 2011; in final form, April 11, 2011

Abstract—Observations of various types of objects in the northern sky were obtained at 44 GHz in the $7_0–6_1A^+$ methanol line on the 20-m Onsala radio telescope (Sweden), in order to search for Class I methanol maser emission in the interstellar medium: regions of formation of high-mass stars, dust rings around HII regions, and protostellar candidates associated with powerful molecular outflows and Galactic HII regions. Seven new Class I methanol masers have been discovered toward regions of formation of high-mass stars, and the existence of two previously observed masers confirmed. The following conclusions are drawn: (1) neither the association of a bipolar outflow manifest in the wings of CO lines with a high-mass protostellar object (HMPO) nor the presence of thermal emission in lines of complex molecules are sufficient conditions for the detection of Class I methanol emission; no association with HMPOs radiating at 44 GHz was found for EGOs (a new class of object tracing bipolar outflows); (2) the existence of H_2O masers and Class II methanol masers in the region of a HMPO enhances the probability of detecting Class I methanol emission toward the HMPO; Class II methanol masers with stronger line fluxes are associated with Class I methanol masers.

DOI: 10.1134/S1063772911120080

1. INTRODUCTION

The development of a strategy for searching for Class I methanol masers (MMIs) remains problematic. As a rule, observations in maser lines are carried out toward known star-forming regions, with the pointing directions chosen primarily based on two criteria. The targets are either known OH, H_2O (see, for example, [1, 2]), or Class II methanol maser sources (MMIIs) [3, 4], or are IRAS sources with color characteristics corresponding to ultra-compact HII zones (see, for example, [5]).

Since the pumping mechanism is generally accepted to be collisional, the presence of bipolar outflows is an obvious factor enhancing the probability of forming such masers. At the same time, a statistical analysis based on a complete catalog of northern and southern MMIs [6, 7] indicated that only about 20% of these masers were associated with such features. One possible reason for this could be difficulty in identifying specifically flows that stimulate the formation of masers. Mainly very simple diagnostics were used, such as the wings of CO or CS lines, i.e., of molecules that trace dense, high-velocity gas.

Another tracer of bipolar flows was proposed in [8]—extended emission in the 4.5-μm band, produced by excited H_2 and CO molecules in shock models. This view was supported in [9]: images obtained in the Galactic Legacy Infrared Mid-Plane Survey Extraordinaire (GLIMPSE) [10] formed the basis for distinguishing a new class of Extended Green Objects (EGOs), comprised of more than 300 extended sources with excesses of green light in the 4.5 μm band in three-color images obtained with the Infrared Array Camera (IRAC) on board the Spitzer space telescope (http://www.spitzer.caltech.edu/).

Approximately two-thirds of EGOs are associated with known MMIs according to the estimates of [11], and slightly fewer—roughly 30%—according to estimates based on a complete catalog of MMIs [6, 7].

At the same time, a survey of 20 EGOs found in GLIMPSE in the 6.7 and 44-GHz methanol lines carried out with high resolution on the Very Large Array [12] yielded an unprecedentedly high rate of identification between EGOs and methanol masers, close to 100%. The MMI emission is more "smeared," and corresponds to more extended emission at 4.5 μm. This supports the idea that EGOs are tracers of bipolar outflows in the early stages of formation of massive stars. In essence, this was the first attempt to search for methanol maser emission using a new criterion,

*E-mail: grosh@asc.rssi.ru

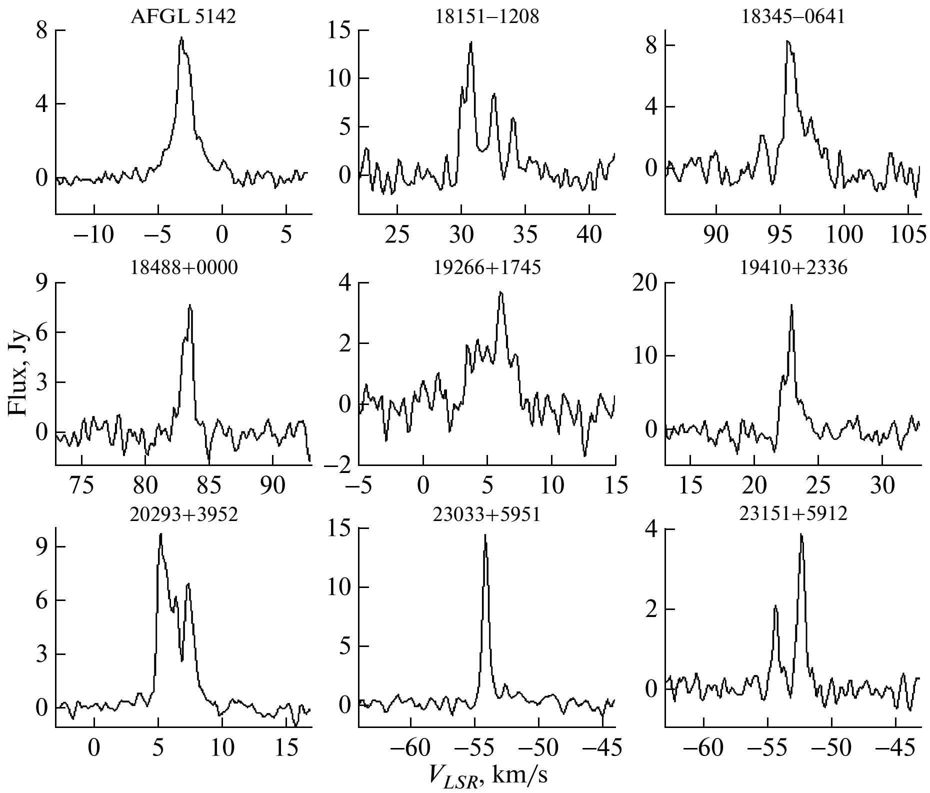

New MMIs radiating at 44 GHz (see text for more information).

based on the characteristics of the studied regions in the near infrared.

In spite of the fact that bipolar outflows should be fairly typical for star-forming regions, far less positive results were obtained from the new, extensive methanol-line survey of 296 regions of formation of massive stars of Fontani et al. [13], carried out at 44, 95, and 6.7 GHz. In this survey, the target regions were chosen to have high luminosities and color relationships in the far infrared [14] characteristic of dense clumps in molecular clouds. Fewer than 20% of the 296 sources are associated with MMIIs, and only about 31% of 88 sources randomly selected from part of this list are associated with MMIs.

In our current study, we present a survey of regions of formation of massive stars carried out at 44 GHz with the aim of searching for new MMIs. A description of the means used to select the target objects is presented below.

2. OBSERVATIONS

The observations were obtained on the 20-m Onsala radio telescope (Sweden) on December 2–15, 2009 at a rest frequency of 44 069.4900 MHz in the $7_0{-}6_1A^+$ methanol line. The beamwidth of the Onsala radio telescope at 44 GHz is 88″. The aperture efficiency is 53%, which corresponds to roughly 18 Jy per Kelvin of corrected antenna temperature. The spectrometer used was a 1600-channel autocorrelator with a transmission bandwidth of 20 MHz and a frequency resolution of 25 kHz, or 0.18 km/s at 44 GHz. The calibration was carried out using a standard chopper-wheel method, including the calculation and application of second-order corrections [15]. The receiver noise temperature was 50 K and the system noise temperature during the observations ranged from 175 K and up, depending on the hour angle and weather conditions. The observations were conducted in an ON–ON regime with position modulation.

3. SELECTION OF TARGET OBJECTS

We used the following four lists for the survey.

(1) Candidate high-mass proto-stellar objects (HMPOs) in an early stage of their evolution from Sridharan et al. [16]. These are objects from the IRAS catalog that (i) were detected in a survey of dense gas radiating in the CS(2-1) lines in regions of formation of massive stars [17], (ii) satisfy the criterion of Wood and Churchwell [18] for selecting ultra-compact HII regions based on their colors in the FIR, (iii) are bright in the FIR ($F_{60} > 90$ Jy and $F_{100} > 500$ Jy), and (iv) were not detected in a survey of the Galaxy at

5 GHz with flux levels higher than 25 mJy; i.e., they do not contain their own ultra-compact HII regions and are isolated from other HII regions.

(2) Regions with massive molecular outflows from Qin et al. [19] that are associated with ultra-compact and compact HII regions.

(3) Proposed regions of formation of second-generation stars from Deharveng et al. [20], in the form of isolated HII regions with simple morpholgies that are located fairly far from the Galactic plane and contain a nearly spherical HII region around an exciting star or cluster, a dust ring surrounding ionized gas that radiates in the mid-IR and millimeter, or a point source from the list of point sources for the "Midcourse Space Experiment" project in the direction of a dust ring.

(4) Regions of formation of massive stars from Qiu et al. [21] containing young high-luminosity ($L > 10^3 L_\odot$) objects associated with molecular outflows.

We selected 35 of 69 objects in the first list, 12 of 15 in the second list, 9 of 17 in the third list, and 3 of 9 in the fourth list for our 44-GHz study.

4. RESULTS

Some 44 GHz detections were obtained for objects from the first list (eight masers were detected, two of which were observed earlier at 95 GHz, and were therefore already known as MMIs) and the fourth list (three masers were detected, two of them also in the first list [16]). The Gaussian parameters of all the new maser sources are presented in Table 1. Spectra of the new methanol masers are presented in the figure, as well as in Figs. E-2, E-3 and E-4, the latter three presented in electronic form at the site http://www.asc.rssi.ru/Lit/online2.pdf. By means of illustration, we present images of three regions for which 8-μm Spitzer IRAC data are available.

The pointing coordinates and velocities for sources for which no 44-GHz emission was detected at the 3σ level are presented in Tables 2 and 3. We also collected a set of 8-μm Spitzer images, including some of objects without 44-GHz detections, presented online in Figs. E-5–E-16 at the site indicated above. MMI emission was not detected in either bipolar outflows near ultra-compact HII regions (the second list, i.e., sources from [21]) or in fragments of molecular clouds adjacent to HII regions (the third list, i.e., sources from [20]).

4.1. Commentary on Individual Sources

1. **IRAS 05274+3345, AFGL 5142**. This is a new 44-GHz maser. A blend of several MMI lines was detected in the narrow velocity interval from −4.2 to 0.5 km/s; one of these is narrow and bright and appears to be a maser feature, while the others may be weak maser or quasi-thermal lines. CS(2-1), H_2O maser, OH maser, and MMII lines are observed in this direction (see the lists in [6, 7]). There are at least three bipolar outflows and one protostellar object in this region, the latter being a candidate high-mass young star [21].

2. **IRAS 18151−1208**. This is a new 44-GHz maser, for which data were previously published in [13]. Four narrow, bright maser lines with widths from 0.37 to 0.84 km/s and fluxes from 6.3 to 8.8 Jy were detected in the narrow velocity interval from 30 to 34 km/s. According to [16], CS and CH_3CN lines, which are tracers of dense gas, CO and SiO lines, which are tracers of material in the wings of bipolar outflows, a weak H_2O maser (0.8 Jy), and an MMII (50 Jy) are also observed in this region; the centimeter-wavelength flux (free–free emission by ionized hydrogen) is less than 1 mJy [16].

3. **IRAS 18345−0641**. This is a new 44-GHz maser. At least two maser lines with fluxes of 8.1 and 2.8 Jy and widths of about 1 km/s were observed in a velocity interval not exceeding the width of the CS thermal lines. The same molecular thermal lines as for the preceding source are also observed toward this source, as well as a somewhat stronger centimeter-wavelength flux (27 mJy) [16].

4. **IRAS 18488+0000**. This is a new 44-GHz maser. Two maser lines with velocities of 83.3 and 83.6 km/s, widths of 1 and 0.3 km/s, and fluxes of 5.6 and 4.2 Jy were observed. The molecular lines characteristic of the interstellar medium are the same [16]. This is the only new maser from the catalog [16] discovered in our survey that has an appreciable centimeter-wavelength flux (194 mJy).

5. **IRAS 19266+1745**. This is a new 44-GHz maser. A blend of at least five maser lines was detected. These lines have velocities from 3.5 to 7.2 km/s, widths from 0.4 to 0.9 km/s, and flux from 1.7 to 3.7 Jy. A CS line, weak H_2O maser (1.5 Jy), and a weak MMII (1.7 Jy) are observed; the centimeter-wavelength flux is less than 1 mJy, and there are no SiO or CH_3CN lines [16].

6. **IRAS 19410+2336**. This is a new 44-GHz maser, known earlier at 95 GHz [22]. Three maser lines at velocities of 22.2, 22.9, and 23.6 km/s were observed, with widths of about 0.5 km/s and fluxes of 7.9, 17, and 4.3 Jy, respectively. Lines of SiO and CH_3CN, a strong H_2O maser (110 Jy), and

Table 1. Gaussian parameters of the 44-GHz maser lines

Galactic coordinates	IRAS identification	RA(B1950) RA(J2000)	Dec(B1950) Dec(J2000)	Line component number	$\int S_\nu dV$, Jy km/s	V_{LSR}, km/s	Line width, km/s	S_ν, Jy	V_{LSR} (CS line), km/s*	CS line width, km/s*
1	2	3	4	5	6	7	8	9	10	11
174.201−0.07	05274+3345	$05^h27^m30.04^s$	33°45′39.3″	1	2.259(0.198)	−4.248(0.027)	2.071(0.036)	1.024	−3.5	3.5
(AFGL 5142)		$05^h30^m48.00^s$	33°47′53.8″	2	10.226(0.144)	−2.682(0.001)	1.308(0.023)	7.347		
				3	2.042(0.144)	−1.201(0.056)	1.277(0.110)	1.502		
				4	0.779(0.054)	0.435(0.053)	0.801(1.368)	0.913		
18.34+1.772**	18151−1208	18 15 09.09	−12 08 34.3	1	3.295(0.738)	30.031(0.032)	0.373(0.061)	8.298	32.8	3.2
		18 17 57.10	−12 07 22.0	2	10.826(1.008)	30.746(0.028)	0.767(0.093)	8.750		
				3	7.031(0.756)	32.504(0.045)	0.841(0.131)	7.866		
				4	3.774(0.540)	34.059(0.039)	0.558(0.099)	6.354		
25.41+0.105	18345−0641	18 34 35.41	−06 41 08.5	1	8.244(1.170)	95.794(0.046)	0.960(0.100)	8.060	95.9	7.8
		18 37 16.8	−06 38 32	2	5.058(1.242)	97.247(0.216)	1.695(0.413)	2.810		
32.993+0.038	18488+0000	18 48 51.16	00 00 41.6	1	6.255(0.612)	83.307(0.047)	1.013(0.087)	5.795	82.7	5.4
		18 51 24.80	00 04 19.0	2	1.317(0.378)	83.669(0.026)	0.295(0.057)	4.194		
53.032+0.117	19266+1745	19 2 40.23	17 45 41.5	1	0.866(0.288)	3.539(0.057)	0.386(0.134)	2.106	5.0	3.9
		19 28 54.00	17 51 56.0	2	1.464(0.630)	4.270(0.098)	0.638(0.293)	2.160		
				3	1.240(0.612)	5.034(0.125)	0.622(0.289)	1.872		
				4	3.664(0.522)	6.142(0.048)	0.928(0.175)	3.708		
				5	1.038(0.342)	7.233(0.087)	0.560(0.189)	1.740		
59.784+0.064***	19410+2336	19 41 04.5	23 36 54.1	1	3.837(0.558)	22.214(0.035)	0.458(0.067)	7.866	22.4	3.1
		19 43 11.40	23 44 06.0	2	9.224(0.828)	22.894(0.016)	0.510(0.055)	16.992		
				3	2.457(0.900)	23.651(0.073)	0.534(0.230)	4.320		
78.975+0.356	20293+3952	20 29 21.4	39 52 59.1	1	8.300(0.702)	5.388(0.030)	0.817(0.049)	9.540	6.3	3.1
		20 31 10.70	40 03 10.0	2	5.309(0.738)	6.341(0.056)	0.854(0.098)	5.850		
				3	6.608(0.288)	7.532(0.018)	0.936(0.052)	6.624		
78.983+0.349	20293+3952	20 29 24.39	39 53 05.9	1	13.618(1.008)	5.466(0.038)	1.024(0.072)	12.492		
MEC		20 31 13.70	40 03 17.0	2	3.557(0.720)	6.408(0.070)	0.699(0.136)	4.788		
				3	11.124(0.558)	7.463(0.020)	0.986(0.066)	10.602		
110.094−0.067	23033+5951	23 03 19.82	59 51 55.3	1	8.549(0.198)	−54.078(0.006)	0.573(0.017)	14.004	−53.1	3.7
		23 05 25.70	60 08 07.9	2	1.016(0.144)	−52.600(0.000)	0.493(0.000)	1.944		
111.236−1.238	23151+5912	23 15 08.7	59 12 25.2	1	1.197(0.126)	−54.340(0.025)	0.557(0.081)	2.016	−54.4	2.6
		23 17 21.00	59 28 49.0	2	2.689(0.108)	−52.332(0.013)	0.653(0.034)	3.870		

* Data taken from [17].
** Published in [13].
*** Observed earlier at 95 GHz [22].

Table 2. Search for 44-GHz maser emission toward regions of formation of massive stars: non-detections for sources from list 1 [16] and one source from list 4 [21] (marked by an asterisk)

Galactic coordinates	IRAS ID	RA(B1950) Dec(B1950)	Dec(B1950) Dec(J2000)	V_{LSR}, km/s
1	2	3	4	5
173.482+2.446	05358+3543	$05^h35^m51.26^s$	35°44′12.5″	−30.0
		$05^h39^m12.8^s$	35°45′50.6″	
182.416+0.247	05490+2658	05 49 5.23	26 58 52.1	0.8
		05 52 12.9	26 59 33	
192.505−3.212	05553+1631	06 01 7.42	16 32 1.4 46	5.7
		05 58 13.9	16 32 00	
18.657−0.06	18223−1243	18 22 22.22	−12 44 00.8	45.6
		18 25 10.9	−12 42 17	
19.883−0.534	18264−1152	18 26 26.69	−11 52 27.4	43.6
		18 29 14.3	−11 50 26	
32.114+0.094	18470−0044	18 47 02.2	−00 44 34.7	96.5
		18 49 36.7	−00 41 05	
37.553+0.201	18566+0408	18 56 40.93	04 08 03.4	85.2
		18 59 09.9	04 12 14	
39.387−0.141	19012+0536	19 01 17.77	05 36 10	65.8
		19 03 45.1	05 40 40	
51.678+0.719	19217+1651	19 21 44.11	16 51 42.6	3.5
		19 23 58.8	16 57 37	
49.668−0.456	19220+1432	19 22 02.77	14 32 07.3	68.8
		19 24 19.7	14 38 03	
53.634+0.021	19282+1814	19 28 14.85	18 14 32.1	23.6
		19 30 28.1	18 20 53	
59.137−0.111	19403+2258	19 40 19.18	22 58 03	26.7
		19 42 27.2	23 05 12	
59.361−0.208	19411+2306	19 41 10.21	23 06 46.7	29.0
		19 43 18.1	23 13 59	
59.759−0.027	19413+2332	19 41 21.55	23 32 51	20.8
		19 43 28.9	23 40 04	
63.125+0.443	19471+2641	19 47 06.21	26 41 16.6	21.0
		19 49 09.9	26 48 52	
71.892+1.312	20051+3435	20 05 06.5	34 35 51	11.6
		20 07 03.8	34 44 35	
77.926+1.681	20205+3948	20 20 33.74	39 48 25	−1.7
		20 22 21.9	39 58 05	
79.35+0.004	20319+3958	20 31 59.74	39 58 25	8.8
		20 33 49.3	40 08 45	
80.634+0.682	20332+4124	20 33 13.04	41 24 23.8	−2.0
		20 35 00.5	41 34 48	
80.828+0.568	20343+4129	20 34 19.6	41 29 33.1	11.5
		20 36 07.1	41 40 01	
103.876+1.855	22134+5834	22 13 24.31	58 34 11.7	−18.3
		22 15 09.1	58 49 09	
102.804−0.719	22172+5912*	22 17 17.79	55 49 54	−43.3
		22 19 08.99	56 04 58.8	
110.21+2.616	22551+6221	22 55 06.83	62 21 40.7	−13.4
		22 57 05.2	62 37 44	
106.098−0.346	22570+5912	22 57 02.89	59 12 22.3	−46.7
		22 59 06.5	59 28 28	
111.253−0.77	23139+5939	23 13 57.97	59 39 00.2	−44.7
		23 16 09.3	59 55 23	
117.315+3.142	3545+6508	23 54 34.16	65 08 29.2	−18.4
		23 57 05.2	65 25 11	

Table 3. Search for 44-GHz maser emission toward regions of formation of massive stars: non-detections for sources from lists 2 [19] and 3 [20]

Source name	Galactic coordinates for pointing	IRAS or MSX ID	RA(B1950) RA(J2000)	Dec(B1950) Dec(J2000)	V_{LSR}, km/s
1	2	3	4	5	6
S175*	120.341+1.985	IRAS 00243+6427	$00^h24^m18.37^s$	64°27′26.3″	−49.0
			$00^h27^m07.8^s$	64°44′02″	
	120.357+1.956		00 24 28.88	64 25 47.9	−49.0
			00 27 18.4	64 42 23.5	
Y**	124.036+0.061	MSX point source***	00 58 01.34	62 38 35.7	−49.0
			01 01 08.4	62 54 44	
	124.039+0.051	IRAS 00580+6238	00 58 02.43	62 37 59.7	−49.0
			01 01 09.5	62 54 08	
S186*	124.86+0.324	IRAS 01053+6251	01 05 19.18	62 51 53.4	−48.0
			01 08 30.6	63 07 53	
	124.896+0.321		01 05 38.41	62 51 39.9	−48.0
			01 08 50.0	63 07 35.1	
S193*	136.125+2.118		02 43 39.86	61 46 03.9	−46.0
			02 47 36.2	61 58 35.4	
G139*	139.912+0.199	IRAS 03035+5819	03 03 33.07	58 19 20.9	−40.0
			03 07 25.41	58 30 52.3	
Sh212**	155.332+2.599	MSX point source	04 36 37.14	50 22 40.9	0.0
			04 40 27.2	50 28 29	
	155.362+2.614	IRAS 04366+5022	04 36 49.45	50 21 56.1	0.0
			04 40 38.9	50 27 44	
Sh219**	159.351+2.569	MSX point source	04 52 20.88	47 18 13.2	−16.5
			04 56 03.3	47 22 57	
	159.355+2.592	IRAS 04523+4718	04 52 27.25	47 18 52.7	−16.5
			04 56 10.5	47 23 36	
S217**	159.143+3.261	MSX point source	04 54 45.4	47 53 59.5	−19.0
			04 58 30.3	47 58 33	
	159.155+3.304		04 55 00.04	47 54 60	−19.0
			04 58 45.0	47 59 32.5	
Sh230 Z**	173.159−1.305	MSX point source	05 19 45.68	33 55 43.1	−16.0
			05 23 03.7	33 58 31	
	173.175−1.29	IRAS 05197+3355	05 19 51.98	33 55 25.5	−16.0
			05 23 10.0	33 58 13	
G206*	206.562−16.339		05 39 18.05	−01 56 42	10.0
			05 41 49.49	−01 55 17.1	
Sh 241**	180.873+4.092	IRAS 06006+3015	06 00 41.36	30 14 59	−6.6
			06 03 54.0	30 14 49.0	

Table 3. (Contd.)

Source name	Galactic coordinates for pointing	IRAS or MSX ID	RA(B1950) RA(J2000)	Dec(B1950) Dec(J2000)	V_{LSR}, km/s
1	2	3	4	5	6
G189*	189.861+0.507	IRAS 06063+2040	$06^h06^m23.04^s$	20°40′02″	9.0
			$06^h09^m21.9^s$	20°39′27.6″	
G213*	213.882−11.836	IRAS 06084−0611	06 08 24.55	−06 11 12	10.0
			06 10 50.99	−06 11 54.1	
Sh 259**	192.909−0.626	IRAS 06084+1727	06 08 29.04	17 27 12.4	22.4
			06 11 23.7	17 26 29.0	
G192*	192.599−0.05	IRAS 06099+1800	06 09 58.16	18 00 12.1	10.0
			06 12 53.32	17 59 22.1	
S288*	218.739+1.848	IRAS 07061−0414	07 06 09.9	−04 14 17.5	57.0
			07 08 38.8	−04 19 08	
	218.723+1.862		07 06 11.08	−04 13 00	57.0
			07 08 40.0	−04 17 50.6	
Sh 104**	74.761+0.618		20 15 49.47	36 36 01.9	0.0
			20 17 42.0	36 45 25	
	74.792+0.579	MSX point source	20 16 04.05	36 36 15	0.0
			20 17 56.6	36 45 39	
X**	77.439+1.716	MSX point source	20 18 57.56	39 25 39.8	0.0
			20 20 46.1	39 35 14	
	77.435+1.706		20 18 59.54	39 25 08.6	0.0
			20 20 48.1	39 34 43	
S138*	105.627+0.338		22 30 52.68	58 12 47.9	−52.0
			22 32 45.7	58 28 16.7	
S149*	108.377−1.036		22 54 14.59	58 16 36	−52.0
			22 56 18.0	58 32 38.3	

* Qin et al [19].
** Deharveng et al. [20].
*** MSX point source.

strong MMII (30 Jy) are observed. The centimeter-wavelength flux is about 1 mJy [16]. As was shown by observations in the IRAC bands [21], as well as other molecular-line and continuum data (see [21] and references therein), this region has a very complex morphology: the IRAS source is surrounded by an elliptical nebulosity whose major axis coincides with the axis of a bipolar outflow; the object that is the source of the bipolar outflow is embedded in a dusty core.

7. **IRAS 20293+3952**. This region is an ultra-compact HII region surrounded by a cluster of young stars or protostellar objects with bipolar outflows (see [21, 23] and references therein). This is a new 44-GHz maser. We obtained observations at two points—at the western edge of the ultra-compact HII region (and offset from this pointing by half a beam), and at the center of the easter methanol emission clump, where the maximum thermal methanol emission has two peaks. Three maser lines at 5.4, 6.3, and

7.5 km/s with widths of about 0.85 km/s and fluxes of 9.5, 5.9, and 6.6 Jy, respectively, were detected toward the edge of the ultra-compact HII region. Methanol maser lines are also present toward the methanol emission clump, at the same velocities and with roughly the same line widths and brightnesses. According to the data of [16], there is also thermal emission in SiO and CH_3CN lines in this region, as well as a bright H_2O maser (100 Jy), but no MMIIs have been detected. The centimeter-wavelength flux is 7.6 mJy.

8. **IRAS 23033+5951**. This is a new 44-GHz maser. Two maser lines at velocities of −54.0 and −52.6 km/s with widths of 0.5 km/s and fluxes of 14 and 2 Jy were detected. A weak H_2O maser (4 Jy) is observed, and there are no MMIIs. There are also no thermal CH_3CN lines. The centimeter-wavelength flux is 1.7 mJy [16].

9. **IRAS 23151+5912**. This is a new 44-GHz maser. Two MMI lines are observed, at velocities of −54.3 and −52.3 km/s, with widths of 0.6 km/s and fluxes of 2 and 3.9 Jy. CO line wings are observed, but there are no thermal CH_3CN or CH_3OH lines. There is a bright H_2O maser (60 Jy), but no MMIIs. The centimeter-wavelength flux is below 1 mJy [16].

4.2. Statistical Analysis

Let us consider the regions in the first list in more detail [16], since we have obtained some 44-GHz detections for this list: below, we compare the characteristics of the objects from this list for which 44-GHz maser emission has and has not been detected.

Sridharan et al. [16] selected 69 candidate HMPOs, using the IR flux (i.e., the dust luminosity and temperature), radio continuum emission at 3.6 cm and 1.2 mm, and molecular-line data as their selection criteria. All 69 objects have 1.2-mm emission, while 3.6-cm radio emission is very weak or absent; this suggests the absence of a developed ultra-compact HII region, implying that the objects are young.

We used some data presented in [16], data from new studies of regions of formation of massive stars from [13], and our own observations, for objects common to these three studies. We were able to carry out such an analysis for 37 of the 69 objects (54%): 34 objects that were studied in our 44-GHz survey in the MMI $7_0{-}6_1A^+$ line, plus three MMIs that were included in the survey of Fontani et al. [13].

Thus, we carried out a statistical analysis for 54% of the sources from the list of Sridharan et al. [16]: 13 44-GHz sources (19%) and 24 non-44-GHz sources (35%). Of the 37 sources included in our analysis, 35% have 44-GHz detections and 65% do not.

Most importantly, we note that CO(2-1) molecular line wings are observed in 35 sources: in all the sources without 44-GHz emission, with only two exceptions. The CO line wings are characteristics of the presence of bipolar outflows, which, as was noted above, can stimulate the formation of MMI emission via collisional pumping. This effect is apparently insufficient, and the maser regions with MMI emission must have some additional characteristics. At the same time, data for nine regions of formation of massive stars studied in [21] indicated that the presence or absence of bipolar outflows according to the Spitzer IRAC data was a critical factor: of these nine sources, eight regions have MMI emission at 44 GHz (see our survey, the survey of Fontani et al. [13], and the MMI catalog [6, 7]), and only one, IRAS 22172+5549, which does not have bipolar outflows, does not have such emission (Table 1; see also [13]), in spite of the fact that the associated CS [24] and CO [13] lines have wings.

It is also interesting that only two sources of the 19 that are in the region of the EGO catalog [9] (8 with and 11 without 44-GHz detections) are EGOs. Both sources (18264−1152 = EGO 19.88−0.53 and 19012+0536 = EGO 39.39−0.14) gave no detection of 44-GHz emission in our data.

MMII emission forming via radiative–collisional pumping in protoplanetary disks is not present at the coordinates of MMIs, according to the primary classification of methanol masers [25, 26]. At the same time, in our case, we find the opposite tendency: MMII emission at 6.7 GHz with stronger fluxes (on average 70 Jy) is observed in 9 of 13 MMIs (i.e., in 70% of the total number of sources with 44-GHz detections); among sources without 44-GHz detections, weak MMII emission (on average 3.3 Jy) was observed in only 7 cases, and MMII emission was not detected at all in 17 cases (in 71% of the total number of non-detections at 44 GHz). In other words, the presence of Class II methanol masers may indicate the possible detection of Class I maser emission, as has been pointed out in other studies (see, for example, [3, 27]).

H_2O maser emission is present in 12 of 13 MMIs (i.e., in 92% of cases); it is also present in six sources (25%) and absent in 18 sources (75%) without 44-GHz detections.

Based on the thermal line radiation, and allowing for the fact that there is no information about CH_3CN emission for three MMIs and eight sources without 44-GHz detections, and no information about thermal methanol emission for eight sources in [16], we can state the following. Seven of ten MMIs (70%) and six of eight sources without 44-GHz detections (75%) have thermal CH_3CN line emission, whereas

Table 4. Statistical analysis of the properties of the sources from [16] studied in our 44-GHz survey in the $7_0-6_1A^+$ MMI line with the 20-m Onsala radio telescope

Source	CO(2-1) line wings	ID with an EGO	ID with MMIIs	ID with H_2O masers	CH_3OH/CH_3CN thermal line emission	Degree of evolution* H/L
44-GHz MMIs detected	100%	0%	70%	92%	69%/70%	100%/0%
44-GHz MMIs not detected	92%	8%	29%	25%	50%/75%	100%/0%

Notes: * Criteria used in [13].
Percents are relative to the total number of objects with and without 44-GHz detections; see the text for further explanations and exceptions.

three MMIs and 10 sources without 44-GHz detections have no such emission. Nine sources of 13 (69%) and eight of 16 (50%) have thermal methanol line emission, while four of 13 and eight of 16 do not (there is no information for eight of the sources without 44-GHz detections). The absence of full information about emission in thermal lines for a number of sources in [16] lowers somewhat the uniformity of these statistical estimates. Nevertheless, it is reasonable to conclude that most of the sources both with and without 44-GHz detections have thermal emission in lines associated with complex molecules.

It is striking that seven sources with 44-GHz detections are denoted "H" according to the classification of Palla et al. [14]; i.e., they are more evolved (six were not included in the survey of [13]). Further, 11 sources without 44-GHz detections are denoted "H," and 13 sources were not observed. Note also that there are no sources in [16], which did not use the criteria of Palla et al. [14] to select sources, that would be included in [13] with the notation "L"; i.e., as sources that would be identified with younger objects.

The list of Sridharan et al. [16] contains two sources known earlier as MMIs—IRAS 18182−1433 [5] and, possibly, IRAS 18454−0158 (W43M, [1]) (see also references in [6, 7]). These sources do not appear in the survey of Fontani et al. [13], and we did not include them in our statistics; however, according to the characteristics presented in [16], these first supports the results of our statistical analysis, while the second worsens the statistical results somewhat, since it contains neither H_2O masers nor MMIIs. Note, however, that IRAS 18182−1433 is the only EGO among the objects from the list of Sridharan et al. [16] with a 44-GHz detection.

The results of our statistical analysis are summarized in Table 4. The three sources in which 44-GHz maser emission was detected do not differ visually from the 12 sources without such emission in images obtained with the Spitzer spacecraft, used by us to illustrate the observed regions (see http://www.asc.rssi.ru/Lit/online2). Both regions with and without 44-GHz emission are present in the list of [16].

5. CONCLUSION

We have carried out a search for new Class I methanol maser emission in the $7_0-6_1A^+$ transition at 44 GHz toward sources from four lists composed using various criteria. We have discovered nine new masers (one of which, IRAS 18151−1208, was observed simultaneously in another survey; see details above). Most of these emit in thermal lines that trace dense gas and have weak centimeter-wavelength fluxes, suggesting that they are in a very early evolutionary stage.

The detected spectral features are narrow (<1 km/s, in many cases), confirming their maser nature, and fairly bright, making it possible to study their spatial structure with high resolution with interferometric observations. The velocity intervals for the spectra do not exceed the widths of the thermal lines of, for example, CS, and the centers of the intervals coincide with the corresponding velocities for the CS lines. Consequently, the maser condensations are at rest relative to the molecular cloud in which they formed.

Neither the association of a bipolar outflow manifest in the CO line wings with a high-mass protostellar object or the presence of thermal emission in lines of complex molecules are sufficient conditions for the detection of Class I methanol emission. No association was found with EGOs, which trace bipolar outflows, for massive protostellar objects that either were or were not detected at 44 GHz (apart from two sources without detections).

The presence of H_2O masers and Class II methanol masers in the region of a HMPO increases the probability of detecting Class I methanol emission toward the object, with the MMIs associated with MMIIs with stronger line fluxes.

ACKNOWLEDGMENTS

This work was partially supported by the Russian Foundation for Basic Research (project code 10-02-00147-a), the Basic Research Program of the Division of Physical Sciences of the Russian Academy of Sciences "Active Processes and Stochastic Structures in the Universe," and the Ministry of Education and Science of the Russian Federation Federal Targeted Program "Scientific and Science-Education Staff of Innovative Russia for 2009–2013" (state contracts nos. 02.740.11.0251 and 16.740.11.0155). We thank S.V. Kalenskii for help in preparing the observing proposal, and the staff of the Onsala Space Observatory (Sweden) for the opportunity to observe with the 20-m telescope and for help in carrying out the observations, particularly P. Bergman and R. Hammargren.

REFERENCES

1. A. D. Haschick, K. M. Menten, and W. A. Baan, Astron. Astrophys. **339**, 949 (1989).
2. R. Bachiller, K. M. Menten, J. Gomez-Gonzalez, and A. Barcia, Astron. Astrophys. **240**, 116 (1990).
3. V. I. Slysh, S. V. Kalenskii, I. E. Val'tts, and R. Otrupcek, Mon. Not. R. Astron. Soc. **268**, 464 (1994).
4. S. P. Ellingsen, Mon. Not. R. Astron. Soc. **359**, 1498 (2005).
5. S. V. Kalenskii, R. Bachiller, I. I. Berulis, et al., Sov. Astron. **36**, 517 (1992).
6. I. E. Val'tts and G. M. Larionov, Astron. Rep. **51**, 519 (2007).
7. I. E. Val'tts, G. M. Larionov, and O. S. Bayandina, arXiv:1005.3715v3 [astro-ph.GA] (2010).
8. M. D. Smith and A. Rosen, Mon. Not. R. Astron. Soc. **357**, 1370 (2005).
9. C. J. Cyganowski, B. A. Whitney, E. Holden, et al., Astron. J. **136**, 2391 (2008).
10. R. A. Benjamin, E. Churchwell, B. L. Babler, et al., Publ. Astron. Soc. Pacif. **115**, 953 (2003).
11. X. Chen, S. P. Ellingsen, and Z.-Q. Shen, Mon. Not. R. Astron. Soc. **396**, 1603 (2009).
12. C. J. Cyganowski, C. L. Brogan, T. R. Hunter, and E. Churchwell, Astrophys. J. **702**, 1615 (2009).
13. F. Fontani, R. Cesaroni, and R. S. Furuya, Astron. Astrophys. **517**, 56 (2010).
14. F. Palla, J. Brand, R. Cesaroni, et al., Astron. Astrophys. **246**, 249 (1991).
15. B. L. Ulich and R. W. Haas, Astrophys. J. Suppl. Ser. **30**, 247 (1976).
16. T. K. Sridharan, H. Beuther, P. Silke, et al., Astrophys. J. **566**, 931 (2002).
17. L. Bronfman, L. A. Nyman, and J. May, Astron. Astrophys. Suppl. Ser. **115**, 81 (1996).
18. D. O. S. Wood and E. Churchwell, Astrophys. J. **340**, 265 (1989).
19. S-L. Qin, J-J. Wang, G. Zhao, et al., Astron. Astrophys. **484**, 361 (2008).
20. L. Deharveng, A. Zavagno, and J. Caplan, Astron. Astrophys. **433**, 565 (2005).
21. K. Qiu, Q. Zhang, S. T. Megeath, et al., Astrophys. J. **685**, 1005 (2008).
22. I. E. Val'tts, A. M. Dzyura, S. V. Kalenskii, et al., Astron. Rep. **39**, 18 (1995).
23. A. Palau, R. Estalella, J. M. Girart, et al., Astron. Astrophys. **465**, 219 (2007).
24. R. Plume, D. T. Jaffe, and N. J. Evans II, Astrophys. J. Suppl. Ser. **78**, 505 (1992).
25. W. Batrla, H. E. Matthews, K. M. Menten, and C. M. Walmsley, Nature **326**, 49 (1987).
26. K. M. Menten, Doctoral Thesis (Bonn Univ., 1987).
27. S. Kurtz, P. Hofner, and C. V. Alvarez, Astrophys. J. Suppl. Ser. **155**, 149 (2004).

Translated by D. Gabuzda